Precambrian Research, 14 (1981) 333—361
Elsevier Scientific Publishing Company, Amsterdam — Printed in The Netherlands

PAN-AFRICAN GRANITOID EMPLACEMENT IN THE ADRAR DES IFORAS MOBILE BELT (MALI): A Rb/Sr ISOTOPE STUDY

JEAN-MICHEL BERTRAND[1] * and IAN DAVISON[2]

[1] *Centre Géologique et Géophysique, Université des Sciences et Techniques du Languedoc, 34060 Montpellier Cedex (France)*
[2] *Department of Earth Sciences, Leeds University, Leeds LS2 9JT (Great Britain)*

(Received June 30, 1980; revision accepted January 23, 1981)

ABSTRACT

Bertrand, J.-M. and Davison, I., 1981. Pan-African granitoid emplacement in the Adrar des Iforas mobile belt (Mali): a Rb/Sr isotope study. Precambrian Res., 14: 333—361.

Time and space relationships between Pan-African intrusives in the Iforas belt (north-east Mali) are discussed. On the basis of structures, lithological composition and plutonism, three domains have been defined. These are, from west to east: (1) the Tilemsi accretion domain; (2) the central domain characterized by an early Pan-African tectonism with large-scale basement nappes; and (3) the eastern domain, a later Pan-African trough deposited on continental basement. Domains (1) and (2) are separated by a huge complex batholith. Geochronological results confirm the structural distinctions and the existence of two major events. As shown by Rb/Sr isochron ages, domains (2) and (3) were stabilized 645 Ma ago. While the multistage evolution of the batholith can be bracketed between 614 and 570 Ma, Rb—Sr biotite whole rock pairs give very similar ages which indicates a short time lapse between emplacement and cooling. The initial ratios, in the range 0.705—0.708 are, as in many other batholiths, slightly higher than the mantle growth curve, indicating a complex origin where crust and mantle are involved. As granitoids occupy some 60% of the surface area in the Iforas belt, the Pan-African epoch corresponds to an important crustal addition in the Iforas segment.

INTRODUCTION

Systematic Rb/Sr studies of orogenic plutonic suites of Upper Proterozoic age belonging to the Pan-African thermo-tectonic event (Kennedy, 1964) have been and are still being carried out in many parts of Africa: NW Hoggar (Allègre and Caby, 1972); Nigeria (van Breemen et al., 1977); NE Sudan (Neary et al., 1976); Saudi Arabia (Greenwood et al., 1976); Namibia (Hawkesworth et al., 1979; Kröner, 1979); Morocco (Charlot, 1976). In many cases they show a complex multistage evolution initiated in Upper Proterozoic times (about 1000 Ma ago).

*Present address: Centre de Recherches Pétrographiques et Géochimiques, Case Officielle No. 1, 54500 Vandoeuvre les Nancy, France.

0301-9268/81/0000—0000/$02.50

The geodynamic evolution of the Malian part of the Touareg shield (see Fig. 1) is now well documented and has been recently interpreted in terms of plate tectonics (Black et al., 1979a; Caby et al., 1981). However, the chronology of the tectonic and plutonic events operating between the oceanic

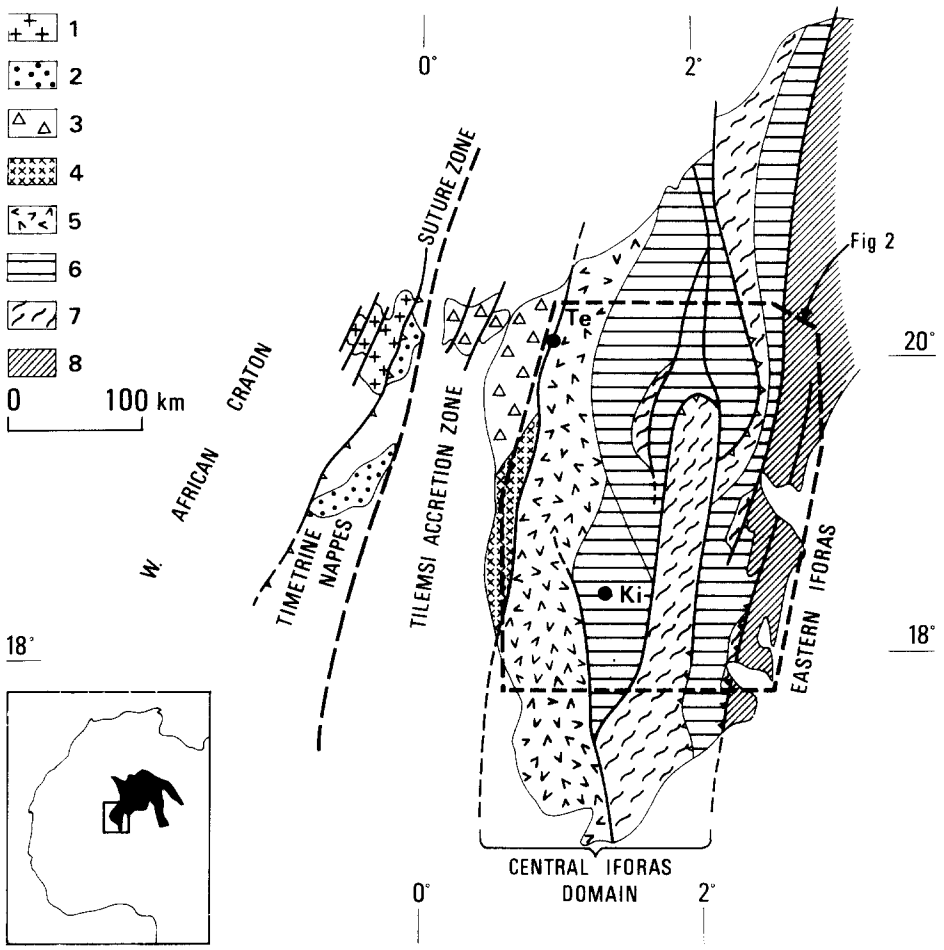

Fig. 1. Sketch map of the Adrar des Iforas. 1: West African craton. 2: HP nappes and ultramafic bodies. 3: Tilemsi accretion zone. 4: LP/HT Aguelhok block. 5: Upper Proterozoic supracrustal formations (Tessalit and Tafeliant formations). 6: Kidal assemblage. 7: Eburnean granulites (Iforas granulitic unit). 8: Eastern domain metasedimentary formations (Tin Zaouatene and Tin Essako). Te: Tessalit. Ki: Kidal.

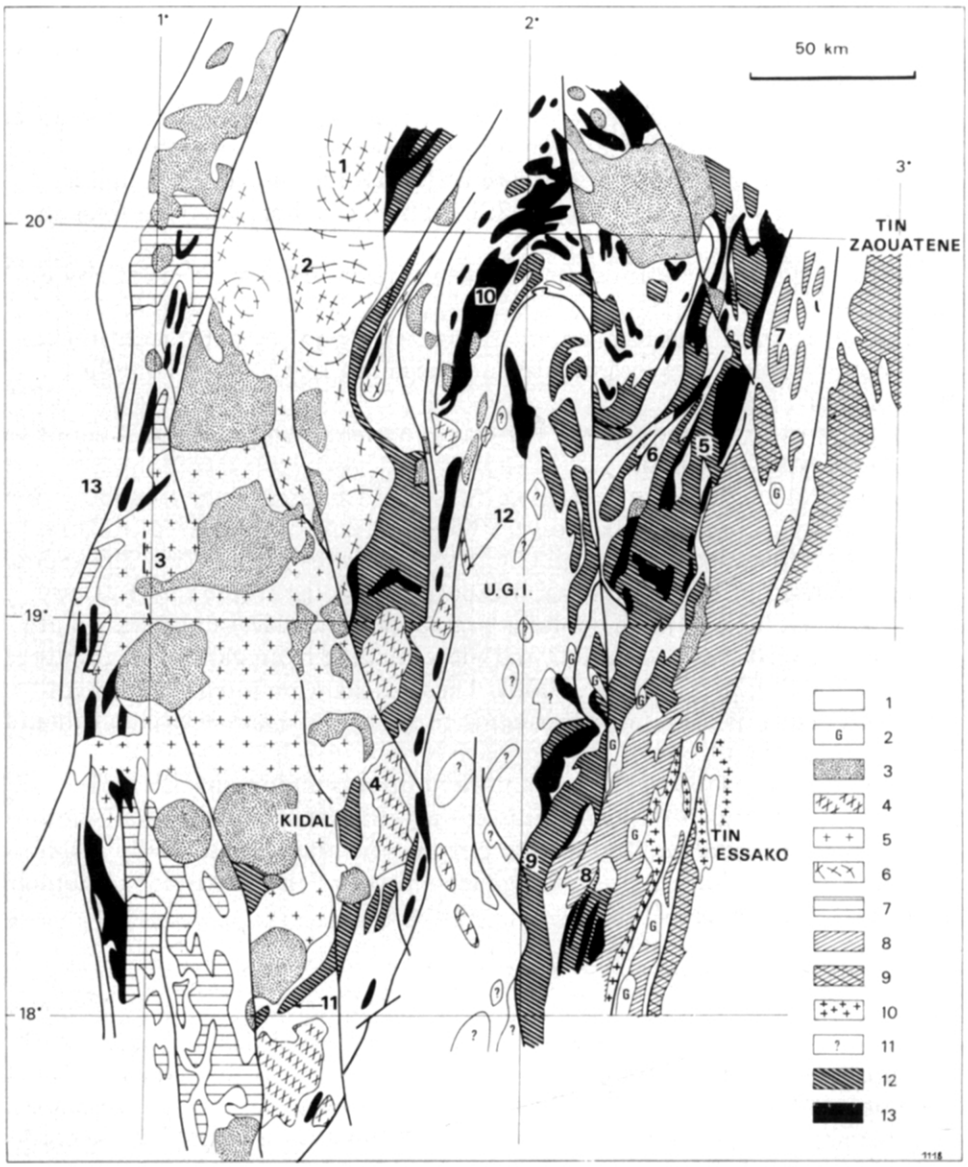

Fig. 2. Distribution of granitoids in Adrar des Iforas. 1: Undifferentiated metamorphic formations. 2: Post-tectonic gabbros. 3: Alkalic ring complexes, post-tectonic bodies and rhyolites. 4: Tedreq type granite. 5: Young batholith: Aoukenek type granite. 6: Old batholith: Tadjoudjemet type granodiorite. 7: Tafeliant intrusives. 8: Eastern domain granitoids. 9: Orthogneisses. 10: Basement (or assumed basement) granitoids from the eastern domain. 11: Undifferentiated Pan-African intrusives within the granulitic unit. 12: Syn- to late-tectonic intrusives of the early Pan-African event. 13: Pretectonic metadiorites. UGI: Iforas granulite unit.

Numbers on the map correspond to sample locations: 1, Tadjoudjemet granodiorite; 2, Oumassène granitoids; 3, Aoukenek granite; 4, Tedreq granite; 5, Achamon granodiorite; 6, Ibedouyen tonalite; 7, Tamassahart granite; 8, Tamaradant granodiorite; 9, Tadaît granodiorite; 10, In Bezzeg metadiorite; 11, O. Teggart tonalite; 12, Abeibara granite; 13, Aguelhok gneisses.

opening, believed to have taken place about 800 Ma ago (Clauer, 1976) and the collision leading to the suturing along the West African craton need some refinement.

Time and space relationships between Pan-African intrusives are discussed from the results of a Rb/Sr isotope study. To simplify the structure of the mobile belt a three-domain classification is proposed here (Figs. 1 and 2). For more details see Black et al. (1979b). These domains are from west to east:

(1) The Tilemsi accretion domain and suture zone (Caby, 1978; Caby et al., in press).

(2) The central Iforas domain, characterized by an early intracontinental evolution involving nappe structure and basement reactivation (Boullier et al., 1978).

(3) The eastern domain, a late Pan-African metasedimentary unit deposited on a continental basement.

Domains (1) and (2) are separated by a N—S trending shear zone bounded to the east by a composite batholith (200 × 40 km) of mainly calc-alkalic composition intruded by later alkalic ring complexes (Ly, 1979). The accretion domain is not discussed here; it is currently being studied by R. Caby and C. Dupuy. This domain contains pretectonic intrusives exhibiting a progressive eastward increase in K_2O and SiO_2, ranging from gabbro to granodiorite (R. Caby, pers. comm., 1980). These rocks were intruded into volcanic and volcanoclastic units belonging to an arc-type and active continental margin environment.

Approximately 60% of the present-day outcrop in domains (2) and (3) is occupied by Pan-African granitoids in which there is an overall evolution from diorite and granodiorite to porphyritic granite and finally alkalic granite. A companion paper on the geochemistry of the granitoids in domains (2) and (3) is in preparation.

ANALYTICAL METHODS

Whole-rock Rb/Sr ratios were determined on pressed powder pellets with a Philips 1212 X-ray fluorescence spectrometer using the procedure of Pankhurst and O'Nions (1973). A spiked internal standard was always present to monitor any drift in count rate, and sample counts were normalised accordingly. Observed drift corrections were negligible relative to the counting statistics (about 0.5%). Estimated average precision on the Rb/Sr ratios is ±1% (2σ), but the Rb and Sr contents are probably only known to ±2%. The following average Rb/Sr ratios were determined on international standards: GSP-1, 1.08; AGV, 0.102; BCR-1, 0.143; G-2, 0.350.

Strontium was extracted using conventional dissolution and ion-exchange techniques for which the total chemical blanks were less than 4 ng/sample. The isotopic composition was determined on a VG Micromass 30 mass-

spectrometer with on-line computer facilities. ^{88}Sr ion beams of about 5×10^{-11} Å, short count times, and fast peak switching corrected for dynamic zero effects allow $^{87}Sr/^{86}Sr$ ratios to be measured at the rate of about 250/hour. By measuring 200—350 ratios on each sample, 0.005% precision (two standard errors on the mean) was usually achieved.

However, to take into account possible heterogeneity of the whole-rock powders, and some analytical results with only a 0.015% precision, a mean of 0.01 seems to be a more realistic estimate of the precision which the $^{87}Sr/^{86}Sr$ ratio of any particular sample is known, and that figure is used in the subsequent age calculations.

Results are therefore quoted to ±0.01% (2σ). Isochrons were calculated using the least-squares method of York (1969) and a ^{87}Rb decay constant of 1.42×10^{-11} a^{-1} is used here (Steiger and Jäger, 1977). All errors quoted are at the 2σ level.*

Biotites were separated using standard magnetic and hand-picking techniques and analysed using a mixed-spike procedure. The Rb was extracted on a column of Biorad AG 50-W - X8 200—400 mesh cation exchange resin. Precision of the Rb/Sr ratios is estimated to be ±1%.

THE CENTRAL IFORAS AND EASTERN DOMAINS

The structural relations between these two domains differ between the north of the Adrar des Iforas (Tin Zaouatene) and the south (Tin Essako, see Fig. 2).

In the north, the two domains are separated by an angular unconformity and sometimes by a late fault, whereas in the south there is an apparent structural concordance between the two domains and no observable unconformity.

Geological setting of the central Iforas domain

The structural evolution of the central Iforas domain is described by Boullier et al. (1978), Wright (1979) and Davison (1980) and three major tectonic units have been outlined. Within each tectonic unit the relationships between the intrusives and the deformation phases are similar, except in the granulite unit where the amount of granitoids is much less than in the adjacent units and the relative chronology is still incomplete.

These three tectonic units will now be described.

(1) The structurally lowest unit is the Kidal assemblage, exposed to the west and north of the granulite unit (see Fig. 2).

It is a high-grade interlayering of reworked basement gneisses and granulites, Upper and Middle Proterozoic meta-supracrustals and associated intrusives and migmatites (Boullier et al., 1978; Caby et al., in press). The meta-supracrustals are inferred to be Upper and Middle Proterozoic, from

*Calculation models are adapted from Faure (1977).

lithological correlations with the supracrustal series in the NW Hoggar described by Caby (1970). The Eburnean age of the granulites is also inferred from lithological correlation with similar rocks in the NW Hoggar dated at 2150 Ma by Allègre and Caby (1972) and Lancelot et al. (1976) using the Rb/Sr and U/Pb methods. But the source rocks are older, as suggested by Rb/Sr isochron ages in the range 2900—3300 Ma (Ferrara and Gravelle, 1966; Allègre and Caby, 1972).

The main horizontal (or refolded) foliation which occurs throughout this unit is thought to be the result of nappe emplacement which took place on deep-seated thrust planes. A Pan-African age for this deformation was inferred from the occurrence within the Kidal assemblage of overfolded metasedimentary lenses which are lithologically very similar to the Middle to Upper Proterozoic sequences defined in the Hoggar (Bertrand and Caby, 1978). This assumption is confirmed by a U/Pb 693 ±3 Ma age on zircon (Ducrot et al., 1979) obtained on a pretectonic to early syntectonic tonalitic emplaced in the Kidal assemblage (O. Teggart, location 11 on Fig. 2).

(2) The Iforas granulite unit has been interpreted as a nappe of granulite-facies gneisses lying upon the gneisses of the Kidal assemblage. The basal tectonic contact between this nappe and the underlying rocks is preserved only along the northern and southeastern edges (Boullier et al., 1978; Davison, 1980), whereas younger, lower-grade mylonites bound the unit elsewhere. The Pan-African deformation in this unit of Eburnean granulites is not penetrative and occurs in narrow shear belts (Boullier, 1980). Pretectonic mafic dykes and ultramafic bodies occur in this unit: ultramafic bodies are clearly Eburnean but mafic dykes are post-Eburnean as they cross-cut the cover rocks and were deformed during early Pan-African phases. Scattered Pan-African granitoid bodies belonging to this unit are beyond the scope of this paper.

(3) East of the granulite unit, numerous thrust sheets, which include strongly deformed Eburnean granulites and Middle to Upper Proterozoic platform metasediments, were intensely folded during several phases of deformation. The basis for the dating of these supracrustal metasediments is again lithological correlations with similar rocks described by Caby (1970) in the western Hoggar. This predominantly metasedimentary tectonic pile structurally overlies the main granulite nappe in the northern area (J.M. Bertrand) and rests structurally below the granulites in the south (I. Davison) (Fig. 2). Several major phases of granitoid intrusions have taken place in this tectonic unit.

Geological setting of the eastern domain

The eastern domain is separated from the central Iforas by an unconformity (Boullier et al., 1978) which is well exposed in the northern part (Fig. 2). In the south of Fig. 2 (near Tin Essako) the contact between the two domains is a thrust, and material of the eastern domain is overthrust westwards onto

the central domain. It is of crucial importance to note that the unconformity represents a break between two distinct tectonic cycles because the refolded nappe pile ($F_1 + F_2$) of the central Iforas was eroded before the deposition of the sediments which occupy the eastern domain. Eastward from the unconformity, deformation and metamorphism increase. Late post-metamorphic thrusts separate lithologically and structurally distinct units, the common point between the units being the existence of pre-thrust LP metamorphic assemblages associated with late tectonic granitoids. However, the easternmost unit in the Eastern domain is the structurally lowest unit observed; this unit consists of orthoquartzites, schists and metavolcanics associated with orthogneisses. The presence of kyanite in these rocks indicates either that higher *P* conditions were attained in this zone and/or that this unit corresponds to a different (older?) tectonometamorphic assemblage.

Geochronological results from the central and eastern domain

The only good results obtained were on granitoids associated with the eastern domain tectonic cycle and its probable equivalents in the central domain (D_3 event of I. Davison). On the contrary, older granitoids from the central domain failed to give isochrons (see Table I).

The Tamaradant granite (Fig. 2, locality 8; Fig. 3)

Located in the southeastern part of the central domain, this pluton postdates the F_2 folding (Davison, 1980) but is itself deformed by the Tamaradant shear zone which was rejuvenated during the D_3 event. The pluton is

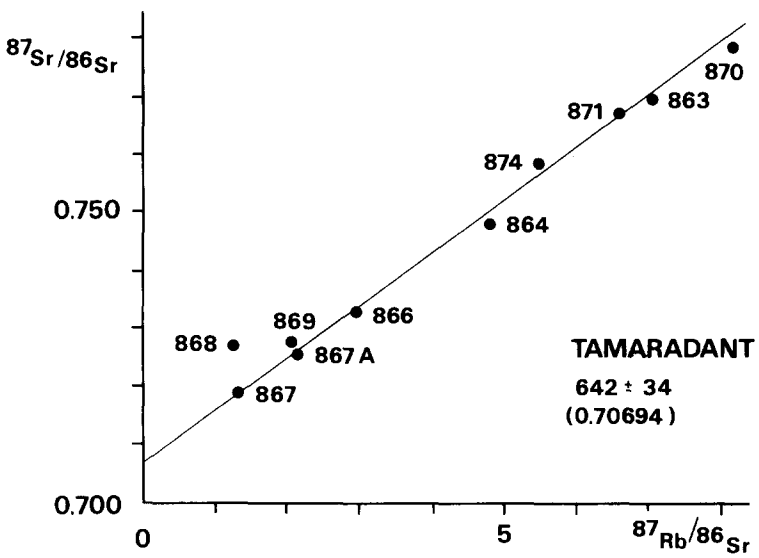

Fig. 3. Rb—Sr isochron diagram of the Tamaradant granodiorites. Mswd = 1 model 3.

TABLE I

Rb—Sr whole rock results

Sample	Area (Fig. 2)	Rb (ppm)	Sr (ppm)	$^{87}Rb/^{86}Sr$ ±2%	$^{87}Sr/^{86}Sr$
(1) Tamaradant granodiorite					
ID 863	8	263	106	7.2217	0.770078 ±70
ID 864	8	127	77	4.7905	0.748360 ±40
ID 866	8	77	76	2.9380	0.733725 ±45
ID 867	8	136	305	1.3010	0.718945 ±100
ID 867 A	8	111	151	2.1304	0.725890 ±15
ID 869	8	130	185	2.0369	0.727838 ±25
ID 870	8	277	99	8.1512	0.779302 ±47
ID 871	8	251	110	6.5542	0.768027 ±300
ID 874	8	223	119	5.4484	0.7588 ±2
ID 868	8	107	252	1.2300	0.7275 ±2
(2) Tamassahart granite					
A 69	7	125	159	2.2796	0.725333 ±83
A 70	7	145	183	2.2974	0.725307 ±128
A 71	7	57	162	1.0185	0.713626 ±448
A 72	7	62.7	168	1.0770	0.714003 ±144
A 73	7	67.7	109.5	1.1569	0.714218 ±231
A 74	7	87	151.5	1.6641	0.719387 ±243
A 75	7	89	155.5	1.6585	0.719306 ±46
A 76	7	65	176	1.0696	0.714174 ±217
A 77	7	57.5	151	1.1029	0.714394 ±59
A 78	7	87	176.5	1.4280	0.716754 ±97
(3) In Bezzeg metadiorite					
N 185	10	42	404	0.3025	0.708073 ±58
N 186	10	54	677	0.2324	0.708424 ±53
N 187	10	11	147	0.2214	0.706065 ±37
N 188	10	46	639.5	0.2078	0.706797 ±40
N 189	10	33.5	650	0.1491	0.707455 ±73
N 190	10	39.5	742	0.1534	0.707170 ±31
N 191	10	32	710.5	0.1308	0.707073 ±42
A 112	10	32	693	0.1336	0.706940 ±85
A 113	10	34	604	0.1630	0.706786 ±348
A 115	10	33.5	679	0.1427	0.706353 ±109
(4) Tadait granodiorite					
ID 853	9	33	703	0.1376	0.706373 ±40
ID 854	9	42	668	0.1818	0.706729 ±27
ID 855	9	54	835	0.2448	0.707304 ±56
ID 856	9	46	645	0.2075	0.706957 ±36
ID 857	9	37	667	0.1633	0.706519 ±20
ID 858	9	31	692	0.1254	0.706200 ±26
ID 859	9	34	705	0.1397	0.706374 ±31
ID 860	9	29	718	0.1169	0.706268 ±26
ID 861	9	34	677	0.1453	0.706500 ±15
ID 862	9	45	646	0.2000	0.707010 ±21

TABLE I (continued)

Sample	Area (Fig. 2)	Rb (ppm)	Sr (ppm)	$^{87}Rb/^{86}Sr$ ±2%	$^{87}Sr/^{86}Sr$
(5) Ibedouyen tonalite					
A 16	6	78	212	1.0655	0.712716 ±28
A 17	6	49.5	410	0.3492	0.706336 ±213
A 18	6	54	410	0.3812	0.706695 ±103
A 20	6	64	363.5	0.5094	0.707633 ±32
A 22	6	57	402	0.4104	0.706505 ±138
A 23	6	73	306	0.6907	0.709773 ±59
(6) Achamon granodiorite					
A 7	5	70.5	567	0.3599	0.709007 ±50
A 8	5	80	526	0.4403	0.709902 ±92
A 9	5	66	422	0.4528	0.709500 ±69
A 10	5	24	752	0.0923	0.710296 ±84
A 11	5	70	585	0.3464	0.709031 ±104
A 14	5	80	443	0.5228	0.710959 ±102
A 15	5	83	528	0.4551	0.709716 ±134
(7) Tadjoudjemet granodiorite					
N 138	1	63	551	0.3309	0.707293 ±56
N 139	1	179	244	2.1260	0.724104 ±40
N 140	1	236	126.5	5.4426	0.752935 ±97
N 141	1	147.5	544	0.7797	0.713196 ±44
N 142	1	144	606	0.6878	0.712700 ±65
N 143	1	123	466	0.7100	0.713500 ±45
N 144	1	120	518	0.6705	0.712875 ±45
N 145	1	115.5	345.5	0.9666	0.731668 ±88
N 146	1	177.5	226	2.2785	0.742651 ±70
N 147	1	94	546	0.1721	0.709816 ±88
N 148	1	190	201	2.7410	0.727113 ±69
N 149	1	233	122	6.0499	0.755303 ±98
N 150	1	210	179	2.4674	0.732177 ±58
(8) Oumassene granitoids					
ID 152	2	106	502	0.6141	0.710415 ±24
ID 153	2	113	468	0.6986	0.711319 ±13
ID 157	2	91	600	0.4391	0.708960 ±21
N 163	2	128.5	403.5	0.9211	0.712079 ±74
N 164	2	128	372.5	0.9928	0.712754 ±45
N 165	2	128	333	1.1093	0.714402 ±91
N 166	2	101	529.5	0.5514	0.709692 ±73
N 167	2	119.5	469	0.7376	0.711469 ±60
(9) Aoukenek granite					
N 215	3	192	223	2.4936	0.725192 ±32
N 217	3	182	290	1.8146	0.719335 ±71
N 218	3	183	235	2.2576	0.722937 ±37
N 220	3	179	269	1.9283	0.720335 ±182
N 223	3	130	611	0.6175	0.709742 ±54

TABLE I (continued)

Sample	Area (Fig. 2)	Rb (ppm)	Sr (ppm)	$^{87}Rb/^{86}Sr$ ±2%	$^{87}Sr/^{86}Sr$
(10) Tedreq granite					
N 225	4	129	606	0.6168	0.718054 ±82
N 226	4	124	375	0.9586	0.715111 ±126
N 227	4	148	190	2.2582	0.724767 ± 50
N 228	4	167	273	1.7727	0.720874 ±44
N 230	4	87	176.5	1.4280	0.718631 ±105
N 231	4	146	233	1.8161	0.721152 ±42
N 239	4	147	253	1.6837	0.720284 ±49
N 241	4	164	178	2.6710	0.726494 ±32

constituted by pink to grey porphyritic granites which are sharply cut by similar finer grained rocks. The margins of this pluton are steep-sided and deformed with a fabric developed parallel to the margin of the pluton.

The porphyritic rocks are slightly deformed, but an essentially igneous texture is preserved. There is sub-grain development and undulatory extinction of the quartz, the micas are bent and the potassium feldspar phenocrysts are full of tiny epidote crystals. The full assemblage in the porphyritic granites is potassium feldspar — plagioclase — hornblende — muscovite — biotite — epidote ± chlorite ± allanite ± sphene ± apatite ± Fe—Ti oxides. The finer-grained granites are undeformed: they possess a granophyric texture and contain zoned plagioclase—microcline, biotite, muscovite, quartz, sphene and Fe—Ti oxides.

Thirteen samples have been analysed from this complex. Twelve of them define an isochron which corresponds to an age of 642 ±34 Ma with an initial $^{87}Sr/^{86}Sr$ ratio of 0.70694 ±67 (Model 3. Mswd = 1). Ten are of the porphyritic variety and occupy the lower part of the isochron, and three are of the late finer-grained type. The only sample which does not lie on the isochron (ID 868) was much deformed by a D_3 shear zone. Crystallization of new biotite attests to the fact that Rb was probably remobilized during shearing, which may account for this point lying above the isochron.

The age given by the isochron is interpreted as the age of intrusion, as there was no further major heating event in this area, and as it is confirmed by the Rb/Sr age of 645 ±12 Ma on biotite which has formed parallel to the F_3 folds in migmatites produced by the intrusion of the Tamaradant pluton.

The Tamassahart alkali feldspar granite (Fig. 2, locality 7; Fig. 4).

This granite belongs to the characteristic LP stage of the post-unconformity tectonic evolution of the eastern domain. This event is the probable but as yet unproven equivalent of the D_3 event in the central domain.

The granite is leucocratic and has alkalic affinities, and an undeformed tex-

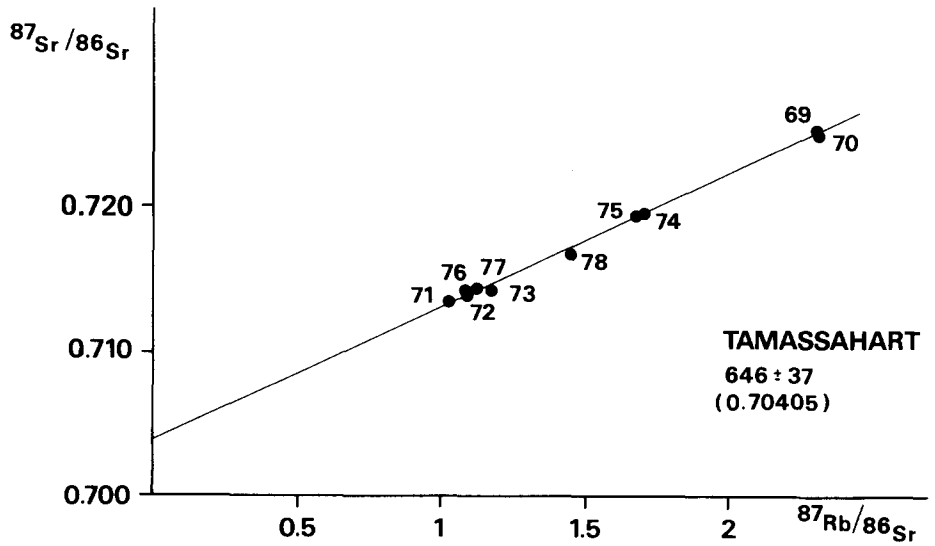

Fig. 4. Rb—Sr isochron diagram of the Tamassahart granites. Mswd = 1,41 model 1 (without samples 73 and 78: Mswd = 0.2).

ture is ubiquitous. The porphyritic members of the Tamassahart granite contain large garnet and cordierite-bearing migmatitic enclaves which are orientated parallel to the N—S trending upright regional foliation; the margins of the pluton are also parallel to this foliation. Three ferromagnesian minerals assemblages have been observed:

(1) Biotite only and then very rich in allanite inclusions.

(2) Colourless hornblende and clinopyroxene with abundant sphene.

(3) Dark brown biotite and blue green hornblende.

Feldspars form a granoblastic assemblage of albite and microcline, but in some samples microcline also forms poikiloblasts. Quartz occurs in rounded recrystallized clusters. Accessories are very abundant; they consist of the following: sphene, acicular apatite, zircon, opaque minerals, allanite. Chlorite is rare, but secondary muscovite is present.

Ten samples of these granites come from two parallel strips which are separated by about 1 km of metasedimentary rocks (A69 and A70 are from the western strip).

All the samples define an isochron with an age of 646 ±37 Ma and an initial $^{87}Sr/^{86}Sr$ ratio of 0.70405 ±60 (model 1. Mswd = 1.41). Two of these samples lie slightly below the isochron, A73—A78 (see Fig. 4) but neither of them exhibits any mineralogical or textural differences from the rest of the suite. Calculation without these points gives approximately the same age (641 ±39 Ma, *Ir* = 0.70426 ±75, model 1. Mswd = 0.2).

Early granitoids from the central domain

The In Bezzeg metadiorites belong to the Kidal assemblage (Fig. 2, locality

10). Completely recrystallized mineral assemblages which reach the amphibolite grade are characteristic of these diorites. No igneous texture is preserved except some recrystallized xenoliths. Rb/Sr measurements produced a cloud on the isochron diagram, but a 650 Ma reference line brackets the possible initial $^{87}Sr/^{86}Sr$ ratio between 0.7065 and 0.7039. A biotite from this diorite gave a Rb/Sr model age of 598 ±10 Ma using an initial $^{87}Sr/^{86}Sr$ ratio of 0:705.

The Tadaït granodiorites (Fig. 2, locality 9; Fig. 5) were syn- or late-tectonically emplaced during F_1 and are strongly deformed by F_2. Relict feldspars have survived F_2 and F_3 deformation, but recrystallization is intense and large poikilitic epidote occurs. Whole-rock data (10 samples) define an isochron with an apparent age of 625 ±81 Ma and an initial $^{87}Sr/^{86}Sr$ ratio of 0.70514 ±7 (model 1. Mswd = 1.24).

The Ibedouyen tonalites and granodiorites (Fig. 2, locality 6; Fig. 6). This pluton occurs in the northeastern part of the central domain and exhibits the same structural relationships as the Tadaït pluton. Its very elongate shape is parallel to the regional foliation, and it is intruded into Upper Proterozoic metasediments. Deformation and recrystallization of the primary assemblage were intense during F_2, but plagioclase phenocrysts survived the deformation. The six analysed samples define an errorchron with an age of 642 ± 84 Ma and an initial $^{87}Sr/^{86}Sr$ ratio of 0.70307 ±78 (model 3. Mswd = 1).

The Achamon tonalites and granodiorites (Fig. 2, locality 5) form composite late-tectonic plutons related to the F_2 folding. Undeformed primary igneous texture is preserved, but widespread chloritization of the biotite has occurred. The seven analysed samples do not define an isochron.

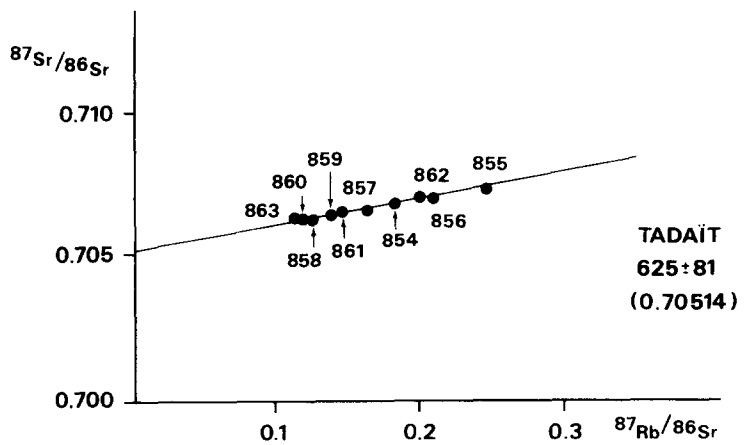

Fig. 5. Rb—Sr isochron diagram of the Tadaït granodiorites. Mswd = 1.24 model 1.

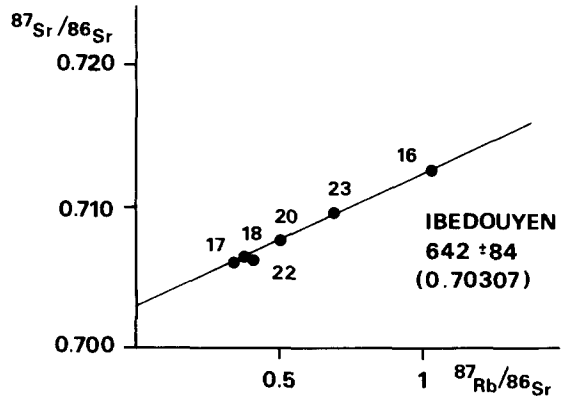

Fig. 6. Rb—Sr isochron diagram of the Ibedouyen granodiorites and tonalites. Mswd = 1 model 3.

Conclusions (Table I)

The ages obtained from the syntectonic granites are too imprecise to determine accurately the age of the F_1 and F_2 phases of deformation in the central domain. The ages obtained by the Rb/Sr method, however, confirm that all these intrusives belong to the Pan-African episode. Deformation and heating events have often re-opened the Rb/Sr system after crystallization of the magmas; however, it may be inferred that these events took place relatively soon after the primary crystallization, as errorchrons can be defined in most cases with all samples falling near to the reference line.

The best results obtained come from the late-tectonic/post-tectonic granites from the eastern part of the central domain and the eastern domain. The similarity of the ages of the Tamassahart and Tamaradant granites suggests that the deformation and metamorphism characteristic of the eastern domain have also affected the southern part of the central domain (where the Tamaradant plutonic complex is situated). The age of about 645 ±30 Ma is that of the major thermo-tectonic event in the central and eastern domain. The basal unconformity of the eastern domain metasediments is thus older than 645 Ma. If R. Caby's contention of the F_1 pre-tectonic character of the O. Teggart tonalite is correct (age 693 ±3 Ma, Ducrot et al., 1979), the early Pan-African event generating the nappe pile and the Kidal assemblage must have occurred between 693 and 645 Ma ago. A further consequence is the short time interval, corresponding to a complete cycle of erosion—sedimentation—deformation—metamorphism and granite emplacement observed in the eastern domain. Such an evolution over a 50 ±30 Ma long period is consistent with modern orogenic belts. Caby et al. (in press) related the early Pan-African event to an early N—S collision whose corresponding suture is postulated to exist in the northwestern part of the Hoggar.

THE MAIN IFORAS BATHOLITH

Geological setting

After the early Pan-African event ending about 650 Ma ago, the resulting tectonized crust collided with the West-African craton. The collision resulted in an E—W shortening of both the Tilemsi accretion domain and the edge of the central Iforas domain. The batholith outlines the western edge of the central domain, already deformed and metamorphosed in early Pan-African times. It was emplaced in several pulses until the end of the E—W shortening of the Iforas massif which is manifested by upright N—S trending folds and vertical shear zones. These folds are especially well developed on the western edge of the batholith within a volcanoclastic formation (Tafeliant and Tessalit) whose relationships with the Kidal assemblage are in question.

The western limit of the batholith is broadly outlined by the Aguelhok—Tessalit late shear zone. Gravity anomalies in the batholith are positive, suggesting that its roots are not extensive (Ly, 1979). The batholith is unconformably overlain by rhyolites (Nigritian series, J. Fabre and R. Black, pers. comm., 1978) which themselves are cut by the alkalic ring complexes one of which (Kidal) has given an age of 593 ±6 Ma (U/Pb on zircons, Ducrot et al., 1979). The intrusion of the large E—W and N—S trending dyke swarms and the presence of late shear zones indicate that the tectonic forces did not cease to act until the end of the emplacement of the batholith. An E—W section across the batholith will now be described, and comparisons will be made with some other parts of the batholith.

Section along the 20th parallel

This section of the batholith is the most complex but provides a good record of the early stages of its emplacement (Fig. 7). The eastern contact with the Kidal assemblage, with widespread metadiorites, is progressive and defines a sheet structure locally disturbed by vertical shear zones and folding. During a first stage a heterogeneous high-potassium pegmatitic granite complex and associated migmatites cross-cut the S'_1 foliation of the gneisses and metadiorites of the Kidal assemblage but are in turn refolded and deformed by a second phase of folding (F'_2) with subhorizontal axial planes (S'_2). The following stage is marked by the emplacement of granodiorites (Tadjoudjemet granodiorites) along these S'_2 planes. Flow foliation and schlieren structures in the granodiorites are interpreted as the result of post-solidification deformation. A continuous sequence has been observed from highly deformed metadiorites and associated pegmatites to poorly orientated schlieren granodiorites (Tadjoudjemet granodiorites). The ubiquitous flat foliation (S'_2) is again deformed to give either narrow belts of upright folds (F'_3) or large-scale dome-and-basin structure; the core of one of the domes is occupied by a norite—charnockite assemblage. These dense rocks, along with the tabular shape of that part of the batholith, may provide an explanation for

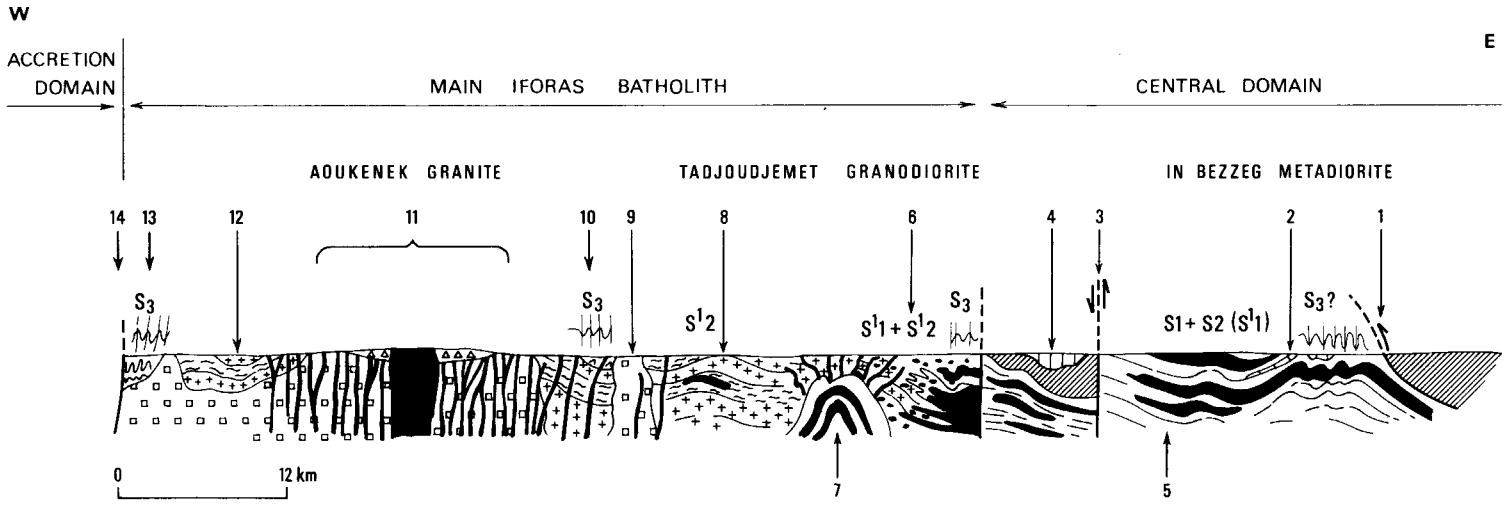

Fig. 7. Schematic composite cross-section of the northern part of the batholith along 20° N. 1: Main thrust contact of the Iforas granulitic unit. A young post-S_3 mylonite belt is neglected here (see Boullier, 1980). 2: Kidal assemblage with metasedimentary lenses and metadiorites (in solid black). 3: Mylonite belt with subvertical lineation. 4: Low-grade upper Proterozoic cover resting upon granulitic basement being progressively reworked downward. 5: Kidal assemblage structurally underlying granulites. 6: S'_1 is deformed (isoclinal F'_2 folds) together with the pegmatitic granite (dots) which themselves crosscut the metadiorites; the sheets of granodiorites (crosses) are interlayered with S'_2 foliation but show a very weak concordant fabric. 7: Tedreq aplites, pegmatites and microgranites. 8: Remnant of the Kidal assemblage. 9: Late porphyritic granite. 10: Andesites of the Oumassène formation (accent) grading into migmatites (waves). 11: Central part of the batholith; Aoukenek type granite (squares) with dyke swarm (microgranites and microdiorites) flat-lying rhyolite flows (triangle) and alkalic ring complex (solid black). 12: Migmatites and sheets of old granodiorites and diorites. 13: Tessalit formation (clastic and volcanoclastic); relationships with the migmatites are unknown.

the positive gravity anomaly centred on the batholith. After the dome formation, porphyritic granites and leucodiorites (Aoukenek granite) were emplaced. Post-tectonic complexes of fine-grained granites and diorites (Tedreq granites), often more or less concentric in shape, and associated with radiating dykes of microgranites, aplites and pegmatites, occur outside the batholith itself; their relation with Aoukenek granite is unknown.

Remnants of basement rocks associated with pretectonic intrusions (mostly metadiorites) have been recognized throughout the whole batholith, suggesting that this batholitic domain as a whole belongs to the reactivated continental block. Furthermore, a migmatitic unit is widely developed in the western half of the section. It grades into metagreywackes, metaconglomerates and metavolcanics and to the andesitic Oumassene Formation. Marbles and basement gneisses together with pretectonic diorites are also associated with these migmatites which were generated during a tectonic episode producing flat-lying foliation (S'_2 ?) which was followed by cross-cutting injection veins of granodiorites. From mappable continuity we interpret this injection stage to be equivalent to the emplacement of the Aoukenek granite. The anatexis and corresponding flat-lying foliation may belong to the same F'_2 post-emplacement evolution of the pegmatitic granite along the eastern edge of the batholith.

Thus, on the basis of this evidence, we distinguish within the batholith:

(1) Remnants of the Kidal assemblage and pretectonic diorites.

(2) The old batholith, composed of pegmatitic granites, migmatites and sheeted granodiorites and related to an F'_2 event.

(3) The young batholith, mostly granitic, in which we can distinguish the central part of the main batholith *s.l.* (Aoukenek granites) and the satellites occurring as isolated concentric plutons east of the main batholith *s.l.* (Tedreq granites) whose time and space relationships are still unknown.

(4) The alkalic ring complexes and post-tectonic subalkalic intrusives with associated dyke swarms not included in this study.

Other areas in the batholith

Further south, in the central part of the batholith, the granites belonging to the young batholith are more extensive. This area is the main location of late orogenic plutonism (work in progress by H. Ba and R. Black). The contacts with the old batholith are often sharp, and the Aoukenek granites (young batholith) show a weak vertical N—S trending fabric which is markedly different from the flat-lying foliation observed throughout the old batholith.

South of Kidal the batholith was not studied in detail. Many rock types and structures are similar, but a striking difference is the fact that the country rocks belong to a semi-pelitic and volcanoclastic sequence (the Tafeliant Formation) whose relationships with the northern Oumassene Formation are unknown. The Tafeliant Formation is affected by upright N—S trending folds whose structural relationships with the F'_2 event (old batholith previous-

ly defined) are still not well known although it is likely to be correlative with F'_3. Granites, tonalites and quartz diorites were syntectonically emplaced during this folding, as suggested by flow structures in the plutons which are parallel to the regional N—S trending structures and to the elongate shapes of the plutons. The whole assemblage is sharply cross-cut, along with development of contact metamorphism, by Aoukenek type granites. An U/Pb zircon age of 613 ± 3 Ma was obtained on one of the Tafeliant syntectonic plutons (Adma tonalites) by Morel (1978) and Ducrot et al. (1979).

Geochronological results

The old batholith

Tadjoudjemet granodiorites and porphyritic granites (Fig. 2, locality 1; Fig. 8a, b). The granodiorites show a weak foliation and layering which define dome-and-basin structures and are cross-cut by porphyritic granites forming irregular homogeneous bodies some kilometres in diameter.

The granodiorites contain feebly zoned plagioclases, biotite, quartz, and poikiloblastic microcline with a small amount of hornblende with rare relict clinopyroxene cores. The cold deformation is taken up by non-penetrative mini shear zones and feeble granulation of the feldspars. The ubiquitous retrogression of biotite to chlorite is also attributed to this later doming effect.

The porphyritic granites are undeformed. They also differ from the granodiorites in that they do not contain hornblende.

As shown on Fig. 8a, the thirteen analysed samples belong to three different granitoid assemblages. It is thus geologically unsound to calculate an age from all of these samples. Samples N147, 148, 149 and 150 come from a heterogeneous western pluton which contains aplogranites and microsyenite together with weakly deformed granites: these samples do not lie on a straight line.

Seven of the samples were taken from the granodioritic domes (N138 to N144). It is these samples which have suffered the most intense post-solidification deformation and which also have the lowest Rb/Sr ratios. They define an isochron with an age of 614 ± 45 Ma and an initial $^{87}Sr/^{86}Sr$ ratio of 0.70628 (model 3. Mswd = 1). N140, which lies very high on the isochron, is an aplitic vein related to N139 and displaying the same fabric. Samples N145 and N146 belong to a late undeformed cross-cutting porphyritic granite. The reference line between these two points gives an $^{87}Sr/^{86}Sr$ initial ratio of 0.722.

Oumassene granitoids (Fig. 2, locality 2; Fig. 9a, b). The samples analysed from the Oumassene area proved to belong to three different bodies. This probably explains the poor alignment of all these points on an isochron diagram. However, five samples (N166, 167, I152, I153, I157) belong to the same undeformed leucocratic tonalite, cross-cutting the youngest folds in the area (F'_3). These rocks give an errorchron with an age of 622 ±129 Ma

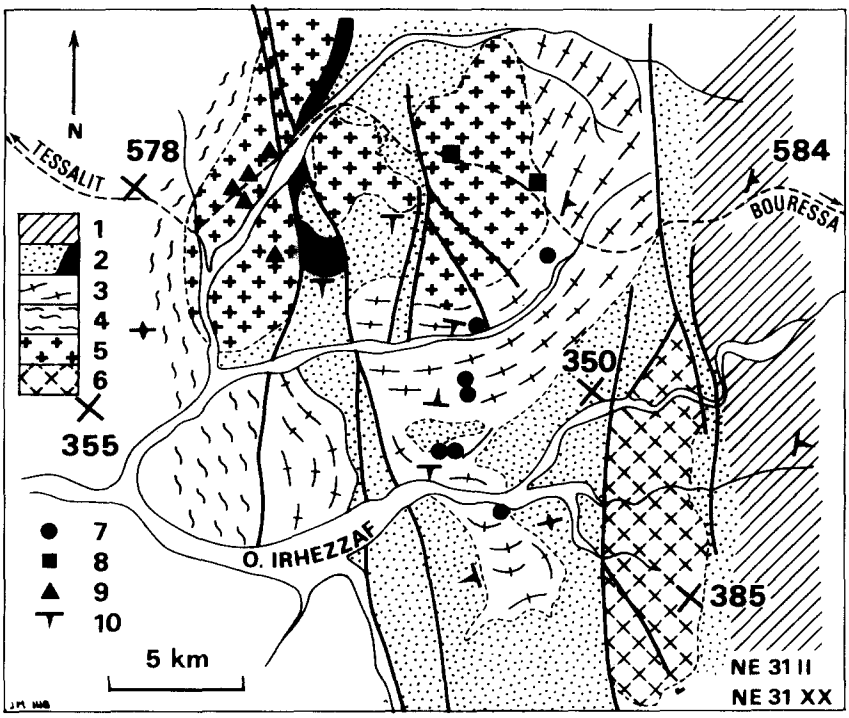

a

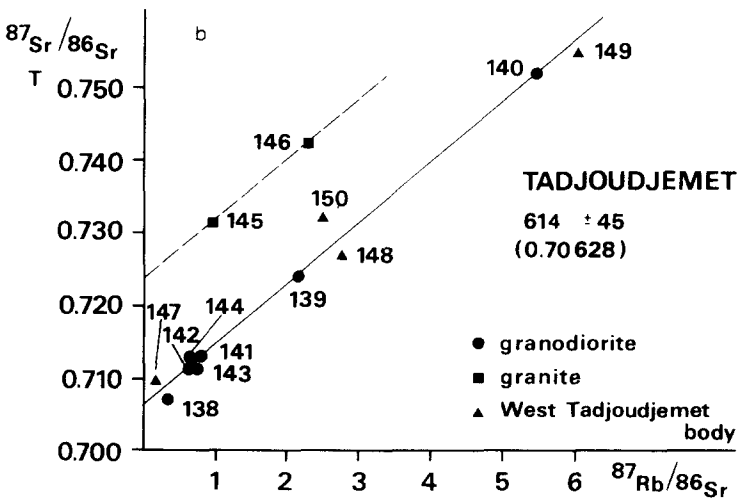

Fig. 8a. Sketch map of the Tadjoudjemet area. 1: Kidal assemblage (mostly metadiorites). 2: Gneisses and metadiorites of the Kidal assemblage invaded by numerous flat-lying aplites and pegmatites; in solid black, metasediments. 3: Granodiorites. 4: Migmatites and heterogeneous granites. 5: Porphyritic granite. 6: Pegmatitic granite. 7: Granodiorites. 8: Porphyritic granites. 9: Granites and quartz monzonites. 10: Foliation. Numbers indicate aerial photographs.

Fig. 8b. Rb—Sr isochron diagram of the Tadjoudjemet granitoids. Mswd = 1 model 3.

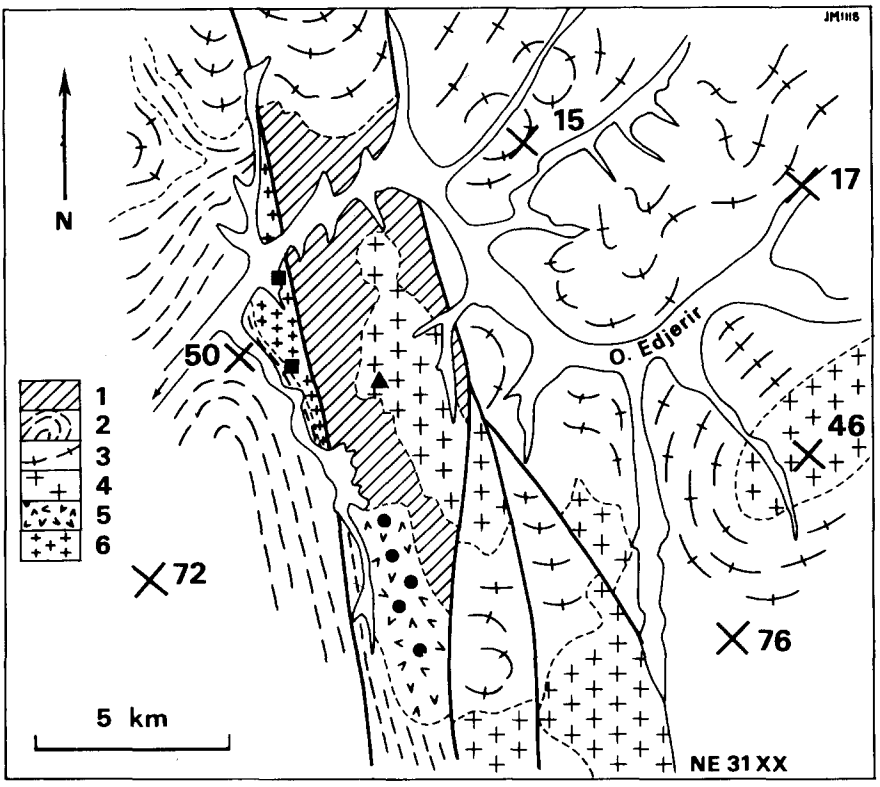

a

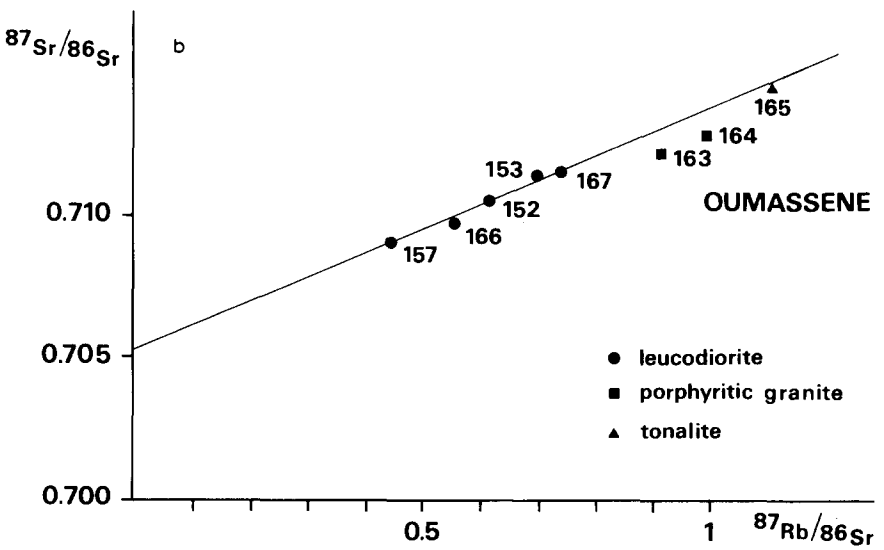

Fig. 9a. Sketch map of the Oumassene area. 1: Migmatites. 2: Andesites of the Oumassene formation. 3: Weakly foliated granodiorites (Tadjoudjemet type). 4: Porphyritic granite. 5: Undeformed leucodiorite. 6: Young granite. Squares: porphyritic granites. Triangles: foliated granodiorites. Circles: leucodiorites. Numbers indicate aerial photographs.

Fig. 9b. Rb—Sr isochron diagram of the Oumassène granitoids.

and an initial $^{87}Sr/^{86}Sr$ ratio of 0.70498 ±113 (model 3. Mswd = 1). A biotite separated from one of the other samples (N164), which suffered a post-emplacement recrystallization and is thought to belong to the old batholith, gave an Rb/Sr model age of 611 ±12 Ma (using an initial $^{87}Sr/^{86}Sr$ ratio of 0.705).

The young batholith

The Aoukenek granite (Fig. 2, locality 3; Fig. 10). The main rock type is a homogeneous, commonly porphyritic biotite granite. Complex oscillatory zoned and twinned plagioclases with albitic rims are associated with either large xenoblastic microcline or subeuhedral poikilitic microcline which are sometimes mantled by albite—oligoclase. Accessory minerals are scarce except for large euhedral sphenes. Biotite is often chloritized, but no evidence of deformation was found except close to the late bordering vertical shear zones. Many shear zones seem to be cross-cut by the Aoukenek granite, but some shearing postdates both the Kidal ring complex and the Aoukenek granite.

Five samples of this granite have been analysed. All five points define an isochron with an age of 570 ±12 Ma and an initial $^{87}Sr/^{86}Sr$ ratio of 0.70471 ±25 (model 3. Mswd = 1). All the analysed samples are homogeneous and similar except N223 which comes from a transition zone (associated with gneissic remnants) and shows evidence of a late magmatic evolution (relict hornblende within biotite). This age is interpreted as the emplacement age.

The Tedreq granite forms one of the eastern satellites of the batholith. It sharply cross-cuts the Kidal assemblage (Fig. 2, locality 4; Fig. 11). This complex lies close to the junction between the reworked Kidal assemblage to the west and the main granulite nappe to the east. It is spatially separated from the batholith (see Fig. 2). Similar plutons have been recognized further

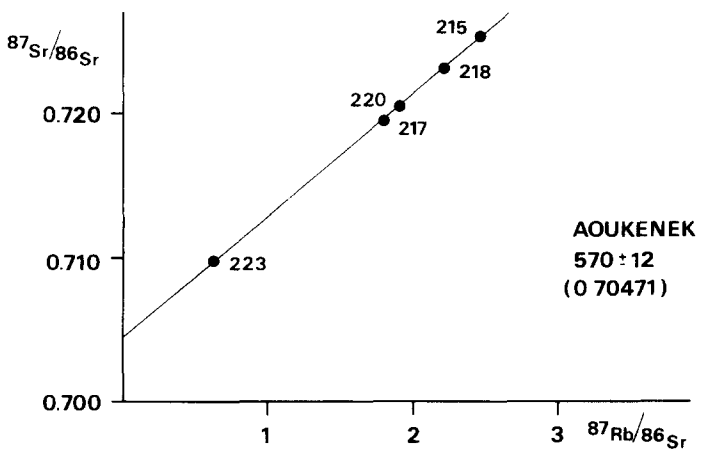

Fig. 10. Rb—Sr isochron diagram of the Aoukenek granite. Mswd = 1 model 3.

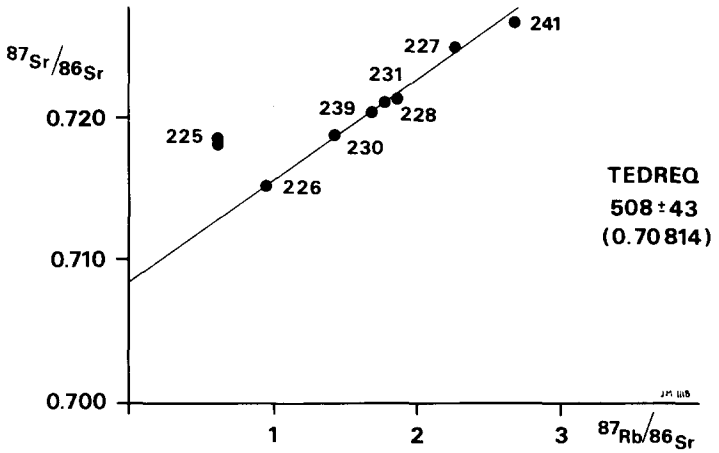

Fig. 11. Rb—Sr isochron diagram of the Tedreq granite. Mswd = 0.4 model 1.

north along a late upright shear zone (Boullier, 1980). Rock types are very homogeneous and are similar in texture and mineralogy to the Aoukenek granite. There are no deformation features present in these rocks. The textures show some subvolcanic tendency with micropegmatites and mantled microcline. The biotite is always slightly chloritized.

Three different areas of the same pluton (40 km long) have been sampled (North N225, 226, 227, 228; centre N230, 231; South N239, 241). Eight samples have been analysed. Six samples define an isochron with an age of 508 ±43 Ma and an initial $^{87}Sr/^{86}Sr$ ratio of 0.70814 ±94 (model 1. Mswd = 0.4). Sample N225 lies well off the reference line. It contains numerous small patches of recrystallized hornblende xenoliths and late N—S trending pegmatite veinlets. Contamination from these two sources is thus very probable. Many xenoliths were also observed in the vicinity of sample N241.

Conclusions (Table II)

The emplacement age of the main batholith can be bracketed between 615 and 570 Ma. These ages are clearly distinct from those of the central and eastern domains although in some instances there is an overlap of errors. The oldest age of 615 ±45 Ma of the Tadjoudjemet granodiorite and 611 ±12 Ma biotite age of the Oumassene granodiorite are similar to the 613 ±3 Ma age obtained by the U/Pb method on zircons in a Tafeliant syntectonic tonalite (Ducrot et al., 1979). Ages are not helpful in differentiating the horizontal regime observed in the old batholith and the upright folding in the Tafeliant Formation. From the structural grounds previously presented one may wonder whether this horizontal regime belongs really to an old batholitic stage as assumed here or to the early Pan-African event (before 650 Ma): if the sample N140 (aplitic vein) is excluded and the sample N138

weighted, an older ill-defined age is possible for the Tadjoudjemet granodiorite. The similarity between the isochron ages and the biotite cooling ages suggests that fast uplift occurred immediately after emplacement and that the Tadjoudjemet and Oumassene granites are relatively high-level bodies. This is in agreement with erosion of the granites having occurred before extrusion of the rhyolites.

There is an inconsistency in the ages of the Kidal ring complex (593 ±6 Ma; U/Pb age of zircons, Ducrot et al., 1979) and of the Aoukenek granite (570 ±12 Ma) because structural grounds indicate that the Aoukenek pluton is older. The very young age of the Tedreq granite (508 ±43 Ma) is a particular case of a localised intrusive event along a major crustal fracture. Along the same mylonite belt (Boullier, 1980), young ages have also been obtained on the Abeibara granite (locality 12 on Fig. 2) using two methods of dating: U/Pb age of zircons giving 566 ±8 Ma (lower intercept on Concordia diagram); and the $^{39}Ar/^{40}Ar$ age giving 539 ±10 Ma (Boullier et al., 1979). However, this body is different in composition and structural evolution from the Tedreq granite as it is deformed by the latest mylonitic event.

DISCUSSION AND CONCLUSIONS

The two stages of stabilization of the Iforas belt (Table II)

One of the purposes of this study was to establish the chronology of the early syntectonic (F_1 and F_2) intrusions which occur in the central domain. This would have been particularly interesting as their relative chronology in relation to the deformation phases had already been formulated. We must admit that this goal was not achieved and that the Rb/Sr method proved unamenable to dealing with plutonic events which produced suites with low Rb/Sr ranges and which were then subjected to greenschist (or higher) facies metamorphism. The time gap between successive syntectonic intrusives proved to be smaller than the error bars produced by the isochrons.

However, the ca. 645 Ma age obtained for the Tamassahart and Tamaradant plutons which, at least for the former granite, postdates the unconformity of the eastern domain formation resting upon eroded $F_1 + F_2$ structures, indicates that the stabilization of the central and eastern domain occurred early in the Pan-African evolution of the belt. Whether or not this first group of events is related to the collision with the West African craton is questionable. Caby et al. (1980) suggested an early collision directed northward, as indicated by the movement direction of the older nappe structures (Caby, 1970, Boullier et al., 1978).

The batholith which corresponds to the leading edge of the overriding eastern continental plate, shows definite differences in age. The 615—570 Ma time-interval corresponding to an old and a young plutonic event generating this batholith is more likely to correspond to the initiation and development of the major collision as proposed by Black et al. (1979a), although flat-

TABLE II

Sequence of Pan-African events in the Iforas segment. Comparison with Morocco (Leblanc and Lancelot, 1980) and NW Hoggar (Allègre and Caby, 1972; Clauer, 1976)

Age (Ma)	Iforas batholith	Central domain	Eastern domain	Comparison with NW Hoggar Anti Atlas Age (Ma)	
510		Tedreq granite		530	In Zize subvolcanic granite (NW Hoggar)
		Mylonites		535	Adoudounian syenite (Morocco)
565		Abeibara granite			
570—590	Aoukenek granite Kidal ring complex (Youth batholith)	Alkaline granites and ring complexes (age unknown)		570	Late granitoids LP metamorphism (NW Hoggar)
	F'_3 Oumassene granitoid (pro parte) Adma (Tafeliant) tonalite			600	B_2 folding (Morocco)
615	F'_2 migmatites and Tadjoudjemet granodiorite (old batholith)				
	Pegmatitic granite			625	Synkinematic granodiorite (NW Hoggar)
645	F'_1 remnants of the Kidal assemblage within the batholith	F_3 Tamaradant granodiorite	Tamassahart granite		
		Kidal assemblage Achamon granodiorite			
		F_2 nappe refolding		680	Early Barrovian metamorphism (NW Hoggar)
		Ibedouyen tonalite Tadait granodiorite	Tin Essako orthogneisses		B_1 folding (Morocco)
690		F_1 O. Teggart tonalite Main nappe emplacement Barrovian metamorphism	(age unknown)		

lying foliations and a tangential regime are characteristic of the early stages of emplacement. Thus the collision process in the Adrar des Iforas (Bayer and Lesquer, 1978; Black et al., 1979a) was not a geologically instantaneous event. It has been shown that similar deformation phases in adjacent domains are not coeval and that all the deformation took place incrementally (Wright, 1979). The following succession of events is proposed for the central and eastern Iforas (Table II):

(1) Polyphase deformation and nappe emplacement in the central domain. The event which affects the Eburnean basement and its Middle to Upper Proterozoic cover is 690 Ma old or slightly younger if compared with the early metamorphism in the "Série à stromatolites" of NW Hoggar (age 685 ±12 Ma by the Rb/Sr method on clay minerals by Clauer, 1976).

(2) Deposition of the Tin Zaouatene Formation followed by N—S trending upright folds (F_3 event; Davison, 1980). These folds were closely linked in

time with LP-type metamorphism and emplacement of the Tamassahart and Tamaradant plutons 645 Ma ago.

(3) Emplacement of the old batholith 615 Ma ago. An unsolved problem lies in the fact that this event (if the same) produced flat-lying structures in the northern part of the batholith and N—S trending upright folds with associated syntectonic intrusives in the southern part of the batholith (Tafeliant Formation).

(4) The evolution then becomes more complex, because although there was still an E—W compressive regime active, there were important N—S lateral displacements which produced large N—S shear zones. However, distension was also present in some regions which permitted dyke swarms and plutons of the Aoukenek type and ring complexes to be intruded at ca. 600—570 Ma ago.

(5) The ultimate events again produced shear zones, some of which may be due to uplift and others to continuing E—W compression. These events have not been studied in detail, but as indicated by Lancelot et al. (in press) and also by the age of the Tedreq granite (508 Ma), the post-orogenic plutonism may have continued in certain places (as in the Hoggar, Boissonnas et al., 1969) right up to the Cambrian.

The cooling history of the belt

Results of the biotite cooling ages are given in Table III. Sample ID487, taken from the Tamaradant batholith, gives the youngest age in the belt (511 ±12 Ma). This is difficult to explain as some 15 km further east (sample ID654) a model age of 645 ±20 Ma was obtained on biotites in migmatites

TABLE III

Rb—Sr biotite results

Sample	Rb (ppm)	Sr (ppm)	$^{87}Rb/^{86}Sr$	$^{87}Sr/^{86}Sr$	How age was derived	Age (Ma)	Locality
N 186	280	13.6	62.63	1.2550 ±6	Bi—WR pair Ir = 0.704	598 ±12	10 In Bezzeg
A 20	335	15.6	65.30	1.2539 ±3	Bi—WR pair Ir = 0.703	595 ±12	6 Ibedouyen
ID 654	563	10.35	184.06	2.4359 ±3	model Ir = 0.75	645 ±12	8 East of Tamaradant
ID 487	584	11	160	1.8681 ±4	model Ir = 0.707	511 ±12	8 Tamaradant
N 164	558	24.08	71.07	1.3221 ±4	Bi—WR pair Ir = 0.704	611 ±12	2 Oumassene
N 139	1108	22	165.23	2.1277 ±6	Bi—WR pair Ir = 0.706	605 ±12	1 Tadjoudjemet
N 242	374	5.34	202.42	2.3790 ±8	model Ir = 0.72	558 ±10	13 Aguelhok

associated with the Tamaradant granites. This enigmatic young age cannot be explained at the present time and further mineral ages would have to be obtained to substantiate it.

If this age is not taken into account, the distribution of the biotite cooling ages, although based on very few points, suggests that the cooling age decreases from 650 ±20 Ma in the east to 560 ±10 Ma in the west, figures which are very similar to those of the whole-rock isochrons.

The two samples analysed from the batholith (Oumassene and Tadjoudjemet) give ages which approximate very closely those of the isochrons. In the same area, but outside of the batholith, the In Bezzeg metadiorite also gives a similar biotite age. Thus both recrystallized old intrusions (In Bezzeg) and high-level (the main batholith) intrusions give similar biotite ages which tends to suggest that there was rapid uplift of the Iforas massif ca. 600 Ma ago. This is further supported by the fact that many mineral assemblages maintain HT minerals which have not undergone retrogression (Davison, 1980).

Origin of the granitoids in the light of the Rb/Sr evidence

The major and trace-element geochemistry of the Iforas granitoids (work in progress) indicate that both the pre-650 Ma intrusives (mostly quartz diorites and granodiorites) and the batholith (with a larger ratio of granites) have calc-alkaline affinities and belong to the I type of White and Chappel (1977), except for the Tamassahart granite which could be the result of the anatexis of supracrustal rocks. The relatively bad definition of the Tamaradant and Tadjoudjemet isochrons may be explained by the scatter of major element contents which may indicate that the samples are not strictly cogenetic.

The range of initial $^{87}Sr/^{86}Sr$ ratios measured in the Iforas varies from 0.722 for two samples of the Tadjoudjemet complex to 0.703 for the Ibedouyen pluton, but the majority of these initial ratios centre around a value of 0.705. All ratios lie above the primitive upper-mantle values one would expect, around 600 Ma ago (Fig. 12), but except for the Tadjoudjemet granitic samples they are far removed from the values one would expect from remelted old continental crust (Faure and Hurley, 1966). The high initial $^{87}Sr/^{86}Sr$ ratio defined by two samples (N145—N146) indicates that they were probably produced from remelted upper crustal material or from a highly contaminated primitive magma. The remelting could be expected in the Tadjoudjemet area due to the tremendous heat influx supplies by the intrusion of the main batholith.

However, in the case of the major part of the granitoids another possibility presents itself in the form of old lower continental crust being the source of these rocks. Certainly within the Iforas massif there are very good candidates for this origin — the Eburnean granulites.

If we consider the only date available for the granulite unit, this comes from the NW Hoggar. Ferrara and Gravelle (1966) state that the granulites

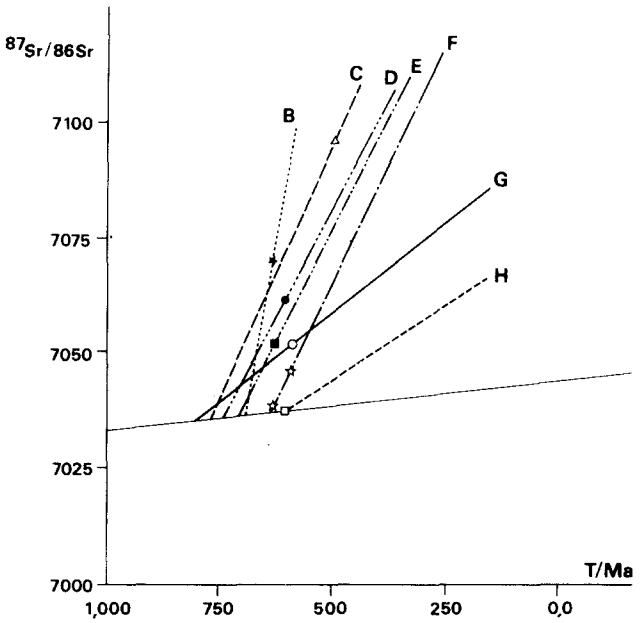

Fig. 12. Sr evolution diagram for the Iforas granitoids. B: Tamaradant. C: Tedreq. D: Tadjoudjemet. E: Tadaït. F: Aoukenek and Tamassahart. G: Oumassène. H: Ibedouyen. The mantle growth line is assumed to be straight and was calculated with a Rb/Sr ratio of 0.02 and a present-day $^{87}Sr/^{86}Sr$ ratio of 0.7045.

have an initial $^{87}Sr/^{86}Sr$ ratio of 0.709 at the time of formation (ca. 2900 Ma ago); this figure thus tends to refute the idea of an old granulite crustal origin. It would seem unlikely that normal convection and conduction sources of heat could melt the amount of granulitic material required to produce the quantity of granites in evidence in the Adrar des Iforas. It would seem reasonable to assume that the granites were not derived from lower crustal granulites but were more probably derived from the mantle. If these granites were derived from the mantle they must have undergone crustal contamination, as all of the granites, with the exception of the Ibedouyen pluton, have initial $^{87}Sr/^{86}Sr$ ratios which fall above the upper-mantle growth line (see Fig. 12).

Figure 12 shows that the earliest time that the magmas could have become chemically segregated from the upper mantle and remained a closed Sr system is about 800 Ma ago. This age is considered by other authors to be the time when ocean opening occurred along the West-African craton margin (Clauer, 1976; Bertrand and Caby, 1978; La Boisse, 1979).

If we exclude melting of a large enough volume of old continental crust to produce granites which occupy 50—60% of the present-day outcrop, the 100 Ma long plutonic history of the Iforas belt could be the result of a continual accretion of granitoid rocks, probably derived from the upper mantle at least 800 Ma ago. Another alternative, considering that early plutonic

bodies are mostly diorites and quartz diorites with low Rb contents, is that of a multistage evolution involving successive remelting of these mantle-derived intrusions. This remelting must have occurred a short time after their emplacement to produce the relatively low initial ratios. This model has to be tested by other methods.

Anyway, even in well studied more recent batholiths, the same problem occurs and more field data and geochemical investigations are necessary for a satisfactory explanation (Pitcher, 1978; Atherton et al., 1979).

ACKNOWLEDGEMENTS

We would like to thank all our colleagues of the Centre Géologique et Géophysique at Montpellier who have contributed to the understanding of the Iforas mobile belt. We acknowledge the cooperation of Drs. M. Dodson and C. Hawkesworth, and also Dr. M. Lasserre and Prof. J. Didier at Clermont-Ferrand who allowed us to use their equipment. I.D. held a U.K. Natural Environment Research Council studentship during the course of this study.

REFERENCES

Allègre, C.J. and Caby, R., 1972. Chronologie du Précambrien de l'Ahaggar occidental. C.R. Acad. Sci., Ser. D, 275: 2095—2098.

Atherton, M.P., McCourt, W.J., Sanderson, L.M. and Taylor, W.P., 1979. The geochemical character of the segmented Peruvian coastal batholith and associated volcanics. In: M.P. Atherton and J. Tarney (Editors), Origin of Granite Batholiths. Geochemical Evidence. Shiva Publishing, Orpington.

Bayer, R. and Lesquer, A., 1978. Les anomalies gravimétriques de la bordure orientale du craton ouest africain. Géométrie d'une suture pan-africaine. Bull. Soc. Géol. Fr. (7), XX, 6: 863—876.

Bertrand, J.M.L. and Caby, R., 1978. Geodynamic evolution of the Pan-African orogenic belt. A new interpretation of the Hoggar shield (Algeria, Sahara). Geol. Rundsch., 67: 357—388.

Black, R., Caby, R., Moussine-Pouchkine, A., Bayer, R., Bertrand, J.M.L., Boullier, A.M. and Lesquer, A., 1979a. Evidence for late Precambrian plate tectonics in West Africa. Nature (London), 278: 223—227.

Black, R., Ba, H., Ball, E., Bertrand, J.M., Boullier, A.M., Caby, R., Davison, I., Fabre, J., Leblanc, M. and Wright, L.I., 1979b. Outline of the Pan-African geology of Adrar des Iforas (Republic of Mali). Geol. Rundsch., 68: 543—564.

Boissonnas, J., Borsi, S., Ferrara, G., Fabre, J., Fabriès, J. and Gravelle, M., 1969. On the early Cambrian age of two late orogenic granites from West central Ahaggar (Algerian Sahara). Can. J. Earth Sci., 6: 25—37.

Boullier, A.M., 1980. L'unité granulitique des Iforas: déformations marginales et interne au cours de l'orogenèse pan-africaine. Rev. Géol. Dyn. Géogr. Phys., 21: 377—382.

Boullier, A.M., 1980. A preliminary study on the behaviour of brittle minerals in a ductile matrix: example of zircons and feldspars. J. Struct. Geol., 2: 211—217.

Boullier, A.M., Davison, I., Bertrand, J.M.L. and Coward, M., 1978. Les granulites du môle des Iforas: une nappe de socle d'âge Pan-Africain précoce. Bull. Soc. Géol. Fr., XX, 6: 877—882.

Boullier, A.M., Ducrot, J., Lancelot, J.R. and Maluski, H., 1979. Influence de la déformation sur le système U—Pb des zircons. Exemple de la bordure ouest de l'Unité Granulitique des Iforas. 7e Reun. Annu. Sci. Terre, Lyon, p. 79.

Caby, R., 1970. La chaîne pharusienne dans le Nord-Ouest de l'Ahaggar (Sahara central, Algérie); sa place dans l'orogenèse du Précambrien supérieur en Afrique. Thèse Etat, Univ. Montpellier, 335 pp.

Caby, R., 1978. Paléogéodynamique d'une marge passive et d'une marge active au Précambrien supérieur: leur collision dans la chaîne Pan-Africaine du Mali. Bull. Soc. Géol. Fr., XX, 6: 857—861.

Caby, R., Bertrand, J.M. and Black, R., 1981. Pan-African ocean closure and continental collision in the Hoggar—Iforas segment, Central Sahara. In: A. Kröner (Editor), Precambrian Plate Tectonics. Elsevier, Amsterdam (in press).

Charlot, R., 1976. The Precambrian of the Anti-Atlas (Morocco): a geochronological synthesis. Precambrian Res., 3: 273—299.

Clauer, N., 1976. Géochimie isotopique du strontium des milieux sédimentaires. Application à la géochronologie de la couverture du craton ouest-africain. Sci. Géol., Univ. Strasbourg, 45, 256 pp.

Davison, I., 1980. A Tectonic Petrographical and Geochronological Study of a Pan-African belt in the Adrar des Iforas and Gourma (Mali). Ph.D. thesis, University of Leeds, 334 pp.

Ducrot, J., La Boisse, H. de, Renaud, U. and Lancelot, J.R., 1979. Synthèse géochronologique sur la succession des événements magmatiques pan-africains au Maroc, dans l'Adrar des Ifras et dans l'Est Hoggar. Xe Coll. Afr. Géol., Montpellier, Abstr. vol., p. 40.

Faure, G., 1977. Principles of Isotope Geology. Wiley, New York, NY, 464 pp.

Faure, G. and Hurley, P., 1966. Isotope composition of Sr in oceanic and continental basalts. Applications to the origin of igneous rocks. J. Petrol., 4: 31—50.

Ferrara, G. and Gravelle, M., 1966. Radiometric ages from the western Ahaggar (Sahara) suggesting an eastern limit for the West African craton. Earth Planet. Sci. Lett., 1: 319—324.

Greenwood, W.R., Hadley, D.G., Anderson, R.E., Fleck, R.J. and Schmidt, D.L., 1976. Late Proterozoic cratonization in southwestern Saudi Arabia. Philos. Trans. R. Soc. London, Ser. A, 280: 517—527.

Hawkesworth, C.J., Gledhill, A.R. and Kramers, J.D., 1979. Nd and Sr isotopes from the Damaran high temperature belt, Namibia. Xe Coll. Afr. Géol., Montpellier, Abstr. vol., p. 45.

Kennedy, W.Q., 1964. The structural differentiation of Africa in the Pan-African (± 500 M.y.) tectonic episode. Res. Inst. Afr. Geol., Univ. Leeds, 8th Annu. Rep., pp. 48—49.

Kröner, A., 1979. Age and evolution of the Pan-African Damara belt of Namibia. Xe Coll. Afr. Geol., Montpellier, Abstr. vol., p. 54.

La Boisse, H. de, 1979. Pétrologie et géochronologie de roches cristallines du bassin du Gourma. Conséquences géodynamiques. Thèse 3e cycle, Univ. Sci. Montpellier, 118 pp.

Lancelot, J.R., Vitrac, A. and Allègre, C.J., 1976. Uranium and lead isotopic dating with grain by grain zircon analysis. A study of complex geological history with a single rock. Earth Planet. Sci. Lett., 29: 357—366.

Leblanc, M. and Lancelot, J.R., 1980. Le domaine pan-africain de l'Anti-Atlas (Maroc). Can. J. Earth Sci., 17: 142—155.

Ly, S., 1979. Etude gravimétrique de l'Adrar des Iforas (Nord-Est Mali). Thèse Doct. ingénieur, Univ. Montpellier, 107 pp.

Morel-à-l'Huissier, P., 1978. Etude paléomagnétique d'une intrusion dioritique pan-africaine dans l'Adrar des Iforas (Mali). Thèse 3e cycle, Univ. Sci. Montpellier, 162 pp.

Neary, C.R., Gass, I. and Cavanagh, B.J., 1976. Granitic association of NE Sudan. Geol. Soc. Am. Bull., 87: 1501—1512.

Pankhurst, R.J. and O'Nions, R.K., 1973. Determination of Rb/Sr and Sr^{87}/Sr^{86} ratios of some standard rocks and evaluation of X ray fluorescence spectrometry in Rb/Sr geochemistry. Chem. Geol., 12: 127—136.

Pitcher, W.S., 1978. The anatomy of a batholith. J. Geol. Soc. London, 135: 157—182.

Steiger, R.H. and Jäger, E., 1977. Subcomission on geochronology. Convention on the use of decay constants in geochronology and cosmochronology. Earth Planet. Sci. Lett., 36: 359—362.

Van Breemen, O., Pidgeon, R.T. and Bowden, P., 1977. Age and isotopic studies of some Pan-African granites from N. central Nigeria. Precambrian Res., 4: 307—319.

White, A.J.R. and Chappell, B.W., 1977. Ultrametamorphism and granitoid genesis. Tectonophysics, 43: 7—22.

Wright, L.I., 1979. The pattern of movement and deformation during the Pan-African in the Adrar des Iforas of Mali. Xe Coll. Afr. Géol., Montpellier, Abstr. vol., p. 77.

York, P., 1969. Least squares fitting of a straight line with correlated errors. Earth Planet. Sci. Lett., 5: 320—324.